Bulgarian Chemical Communications, Volume 51, Issue 4 (pp. 527 - 540) 2019 DOI: 10.34049/bcc.51.4.5041

Investigating the influence of *p*-substituents upon spectral, thermal, kinetic, molecular modeling and molecular docking characteristics of new synthesized arylazobithiazolylhydrazones

N.M. El-Metwaly[1,2*], S. Bondock[2,3], I.I. Althagafi[1], A.M. Khedr[1,4*], A.A. El-Zahhar[3,5], F. A. Saad[1]

[1] *Department of Chemistry, Faculty of Applied Science, Umm Al-Qura University, Makkah, Saudi Arabia*
[2] *Chemistry Department, Faculty of Science, Mansoura University, Mansoura, Egypt*
[3] *Chemistry Department, Faculty of Science, King Khalid University, Abha, Saudi Arabia*
[4] *Chemistry Department, Faculty of Science, Tanta University, Tanta, Egypt*
[5] *Nuclear Chemistry Department, Atomic Energy Authority, Cairo-13759, Egypt*

Received January 7, 2019; Revised May 31, 2019

A series of novel arylazobithiazolylhydrazones **(A-E)** were efficiently synthesized *via* the reaction of thiazolylthiosemicarbazone **3** with hydrazonoyl chlorides **4a-e** in boiling ethanol containing triethylamine as catalyst. The synthesized thiazoleazodye derivatives were characterized by microanalyses and spectral data (IR, $_1$H-NMR and $_{13}$C-NMR), as well as thermal analysis. Moreover, theoretical implementations for compounds (modeling and docking) were taken in consideration. The molecular and structural formulae were established on the basis of analyses and compared altogether in their general features. The influence of substituents on thermal, kinetic, biological activity and reactivity was investigated. The decomposition pathway is completely affected by substituents type. The kinetic parameters estimated have direct relation with the heating rate as well, deeply affected by the inductive effect of substituents. Variable essential parameters were computed upon optimized structures applying Gaussian 09 and Hyper Chem 8.1 programs. In between, the indices attributed to reactivity and biological features point to the priority of compound E in coinciding with the presence of sulfur atom in the substituent group. Also, docking study differentiates between tested derivatives; their behavior in docking efficiency was varied in coinciding with various substituents, as expected. The best docking efficiency was recorded with derivative E, which includes a highly inductive functional group (SO_2NH_2) as *p*-substituent.

Keywords: kinetic study, bithiazolylhydrazones, Gaussian 09 software, molecular docking

INTRODUCTION

The synthesis of heterocyclic compounds has been thoroughly investigated over decades as raising significant interest to their great therapeutic effects and various heterocyclic compounds containing nitrogen and sulfur display elastic structures for drugs improvement [1]. Thiazoles are considered as a heavily studied class of aromatic five-membered heterocyclics which are found in many powerful biologically active drugs such as Sulfathiazol (antimicrobial drug), Ritonavir (antiretroviral drug), Abafungin (antifungal drug) and Tiazofurin (antineoplastic drug) [2]. Thus, thiazole or thiazolyl moiety if it is present in any compound will show numerous biological activities such as anti-inflammatory [3], antimicrobial & antifungal [4], antihypertensive [5], anticancer [6], anti-HIV [7], antidiabetic [8], and anticonvulsant [9] activities. Hydrazone-based compounds represent a very important class of derivatives with a broad spectrum of strong pharmacological influences [10]. A variety of hydrazones were synthesized with potential pharmacological activities like antibacterial, anti-inflammatory, analgesic, anti-hypertensive, antifungal, antiplatelet, antimalarial, anticonvulsant, antidepressant, antiviral, and anticancer [11]. Beside their extensive biological characteristics they also integrate with other active functional groups to display pharmacologically active molecules [12, 13]. For example, thiazolylhydrazones displayed an excellent ability to effectively inhibit leukemic tumor cell growth and to decrease the concentrations of deoxyribonucleoside triphosphate [14]. Furthermore, excessive accumulation of metal ions in brain leads to neurodegeneration. Metal-promotion neurotoxicity is proposed to be attached with various neurological diseases [15]. Recently, chelation therapy has become a significant handling for the symptoms associated with the central nervous system [16]. Different classes of sulfur- and nitrogen-containing compounds are capable to form complexes with metal ions interacting with biological systems [17-19]. Referring to the strong reactivity of the hydrazine nitrogen (C=N) and azo

* To whom all correspondence should be sent:
E-mail: abkhedr2010@yahoo.com
n_elmetwaly00@yahoo.com

(N=N) groups, compounds including both groups represent a versatile class which is significant in curing chemistry [20-23].

On the other hand, thermal methods of analysis are most widely used to study industrially important products such as polymers, pharmaceuticals, metals, minerals, alloys, clays, various metal complexes, etc. [24]. Panchal *et al.* [25] have reported thermo gravimetric analysis of lanthanide coordination polymers with the Schiff base N,N'-di (o-hydroxy phenyl) terephthalaldehyde and determined final decomposition products. Aghera and Parsania [26] have reported thermo gravimetric analysis of symmetric double Schiff bases containing cardo group to understand the effect of different substituents on thermal stability, kinetic parameters of Schiff bases. Recently, Gangani and Parsania [27] have reported thermo acoustical studies of various substituted symmetric double Schiff bases. From researches reported, this work aims to start synthesis of new arylazobithiazolylhydrazone derivatives with various *p*-substituents over one side, and to investigate their influence on the kinetic parameters upon thermal study. The effect of aromatic substituents on the homolysis of organic compounds suffers an observable shortage in literature review. The formulae will be established based on elemental, spectral and conformational optimization software. The docking towards DNA was taken in consideration, to give a comparative view about their inhibition efficiency, which points to their expected efficiency with infected cell DNA.

EXPERIMENTAL

All reagents and solvents used were purchased from Sigma-Aldrich and used without any further treatments.

Techniques of analyses

Using a digital Gallen-Kamp MFB-595 instrument with open capillary tubes, the melting points were recorded and are uncorrected. On Schimadzu FTIR 440 spectrometer using KBr pellets, the IR spectra were determined over range of 400-4000 cm^{-1}. Using a Bruker model 400 MHz Ultra Shield NMR spectrometer through DMSO-d_6 using tetramethylsilane (TMS) (internal standard), the ^{1}H-NMR and ^{13}C-NMR spectra were recorded. Chemical shifts were reported as δ_{ppm} units. The elemental analyses were performed using Perkin-Elmer 2400 CHN Elemental Analyzer. Shimadzu Thermal Analyzer was used to obtain the TGA curves of the complexes applying variable heating rates; 5-25 $K.min^{-1}$, under pure N_2 atmosphere, over the range of 20-900 ^oC. Conformational analysis was executed by Gaussian 09 program and molecular docking by Autodock 4.2 tools. 1-(2-Allylamino-4-methylthiazol-5-yl)ethanone (**1**) and hydrazonoyl chlorides **4a-e** were prepared according to previously reported procedures [28, 29].

Synthesis of 2-(1-(2-allylamino-4-methylthiazol-5-yl) ethylidene)-N-phenylhydrazine-1-thiocarboxamide (3)

A solution of 0.01 mol (1.96 g) of 1-(2-allylamino-4-methylthiazol-5-yl)ethanone **1** was dissolved in 30 mL of ethanol and then 0.01 mol (1.67 g) of 4-phenylthiosemicarbazide was added in presence of 0.5 mL of conc. HCL. The solution was heated under reflux for 4 h, then allowed to cool down to room temperature. The precipitate (compound **3**) was isolated by filtration, washed wth ethanol, dried and recrystallized from MeOH:DMF (1:1) mixture (Scheme 1). Pale yellow powder, Yield (87%), mp 202-203^oC; IR (KBr) ν_{max}/cm^{-1}: 3310 (NH), 3187 (NH), 3036 (NH), 3015 (CH-sp^2), 2930 (CH-sp^3), 1622 (C=C), 1598 (C=N), 1261 (C=S); ^{1}H-NMR (400 MHz, DMSO-d_6): δ_{ppm} = 2.38 (s, 3H, CH_3), 2.52 (s, 3H, CH_3), 4.19 (s, 2H, NCH_2), 5.24 (dd, J_{AB} = 1.2, J_{AC} = 10.4 *Hz*, 1H, =C-H_A), 5.33 (dd, J_{AB} = 1.2, J_{BC} =16.8 *Hz*, 1H, =C-H_B), 5.85-5.94 (m, 1H, =C-H_C), 7.16-7.65 (m, 5H, Ar-H), 9.81 (bs, 1H, NH), 10.43 (bs, 1H, NH), 11.08 (bs, 1H, NH); ^{13}C-NMR (100 MHz, DMSO-d_6): δ_{ppm}= 14.78 (CH_3), 16.66 (CH_3), 47.93 (CH_2N), 117.93 (CH_2=), 120.50 (Thiazole-C_5), 125.50 (CH_{Ar}), 128.73 ($2CH_{Ar}$), 129.19 ($2CH_{Ar}$), 132.63 (CH=), 139.43 (C_{Ar}), 144.64 (C=N), 154.02 (Thiazole-C_4), 166.54 (Thiazole-C_2), 177.03 (C=S); Anal. Calcd. for $C_{16}H_{19}N_5S_2$ (345.11): C,55.63; H, 5.54; N, 20.27%, Found: C, 55.59; H, 5.52; N, 20.26%.

Synthesis of 2-allylamino-4-methyl-5-(1-((4-methyl-3-phenyl-5-(arylazo)thiazol-2(3H)yildene) hydrazono)ethyl)thiazoles (A-E)

Solutions of equimolar amounts of hydrazonoyl chloride **4** (0.005 mol) and compound **3** (1.73 g, 0.005 mol) in 30 mL of ethanol were mixed in presence of 0.5 mL of triethylamine. The mixture was heated under reflux for 3 h, then cooled down to room temperature. The resulting thiazole dye was collected by filtration, washed with aqueous ethanol, dried and recrystallized from glacial acetic acid to afford the aimed compounds **(A-E)**.

2-Allylamino-4-methyl-5-(1-((4-methyl-3-phenyl-5-(4-fluorophenylazo)thiazol-2(3H)yildene) hydrazono)ethyl)thiazole (A). Red crystals, Yield (88%), mp 236-237^oC; IR (KBr) ν_{max}/cm^{-1}: 3200 (NH), 3063 (CH-sp^2), 2989 (CH-sp^3), 1619 (C=C),

1592 (C=N), 1567 (N=N); ^{1}H-NMR (DMSO-d_6): δ(ppm) = 2.52 (s, 3H, CH_3), 2.49 (s, 3H, CH_3), 2.56 (s, 3H, CH_3), 5.17-5.28 (m, 2H, CH_2=), 3.92 (bs, 2H, NCH_2), 5.93 (m, 1H, =C-H_C), 7.17-7.24 (m, 5H, Ar-H), 7.49 (d, *J* = 7.5 Hz, 2H, Ar-$H_{2,6}$), 7.31 (d, *J* = 7.5 Hz, 2H, Ar-$H_{3,5}$), 8.35 (bs, 1H, NH); ^{13}C-NMR (DMSO-d_6): δ_{ppm}= 16.90 (CH_3), 17.36 (CH_3), 19.69 (CH_3), 46.78 (CH_2N), 113.69 (Thiazole-C_5), 116.45 (CH_2=), 116.52 (2CH_{Ar}), 119.29 (Thiazole-$C_{5'}$), 121.55 (2CH_{Ar}), 123.40 (CH_{Ar}), 132.41 (2CH_{Ar}), 134.88 (2CH_{Ar}), 135.21 (CH=), 139.93 (C_{Ar}), 149.29 (C_{Ar}), 150.21 (Thiazole-C_4), 154.27 (Thiazole-$C_{4'}$), 161.52 (C_{Ar}), 168.20 (Thiazole-C_2), 168.98 (Thiazole-$C_{2'}$), 173.56 (C=N); Anal. Calcd. for $C_{25}H_{24}FN_7S_2$ (505.64): C,59.39; H, 4.78; N, 19.39%, Found: C, 59.57; H, 4.75; N, 19.38%.

2-Allylamino-4-methyl-5-(1-((4-methyl-3-phenyl-5-(4-chlorophenylazo)thiazol-2(3H)yildene) hydrazono)ethyl)thiazole (B). Red powder, Yield (95%), mp 234-235ºC; IR (KBr) ν_{max}/cm^{-1}: 3197 (NH), 3082 (CH-sp^2), 2965 (CH-sp^3), 1621 (C=C), 1593 (C=N), 1570 (N=N); ^{1}H-NMR (DMSO-d_6): δ_{ppm} = 2.11 (s, 3H, CH_3), 2.35 (s, 3H, CH_3), 2.40 (s, 3H, CH_3), 3.90 (s, 2H, NCH_2), 5.13 (dd, J_{AB} = 1.6, J_{AC}=10.2 Hz, 1H,=C-H_A), 5.24 (dd, J_{AB} = 1.6, J_{BC}=17.0 Hz, 1H, =C-H_B), 5.86-5.95 (m, 1H,=C-H_C), 7.10-7.39 (m, 5H, Ar-H), 7.41 (d, *J* = 7.5 Hz, 2H, Ar-$H_{3,5}$), 7.67 (d, *J* = 7.5 Hz, 2H, Ar-$H_{2,6}$), 8.05 (bs, 1H, NH), 10.59 (s, 1H, NH); ^{13}C-NMR (DMSO-d_6): δ_{ppm}= 13.59 (CH_3), 16.70 (CH_3), 19.13 (CH_3), 46.55 (CH_2N), 116.24 (CH_2=), 117.32 (Thiazole-C_5), 119.54 (Thiazole-$C_{5'}$), 123.91 (2CH_{Ar}), 128.70 (2CH_{Ar}), 129.81 (2CH_{Ar}), 129.81 (2CH_{Ar}), 129.98 (CH_{Ar}), 132.75 (CH=), 136.15 (C_{Ar}), 140.00 (C_{Ar}), 150.60 (C_{Ar}), 151.79 (Thiazole-C_4), 156.16 (Thiazole-$C_{4'}$), 162.25 (Thiazole-C_2), 167.83 (Thiazole-$C_{2'}$), 173.56 (C=N); Anal. Calcd. for $C_{25}H_{24}ClN_7S_2$ (522.1): C,57.51; H, 4.63; N, 18.78%, Found: C, 57.48; H, 4.60; N, 18.75%.

2-Allylamino-4-methyl-5-(1-((4-methyl-3-phenyl-5-(4-bromophenylazo)thiazol-2(3H)yildene) hydrazono)ethyl)thiazole (C) Red crystals, Yield (90%), mp 240-241ºC; IR (KBr) ν_{max}/cm^{-1}: 3191 (NH), 3082 (CH-sp^2), 2935 (CH-sp^3), 1620 (C=C), 1598 (C=N), 1569 (N=N); ^{1}H-NMR (DMSO-d_6): δ_{ppm} = 2.47 (s, 3H, CH_3), 2.48 (s, 3H, CH_3), 2.55 (s, 3H, CH_3), 3.92 (bs, 2H, NCH_2), 5.16 (dd, J_{AB}= 1.6, J_{AC}= 10.2 Hz, 1H, =C-H_A), 5.25 (dd, J_{AB} = 1.6, J_{AC}= 17.0 Hz, 1H, =C-H_B), 5.91-5.93 (m, 1H, CH=), 7.17-7.24 (m, 5H, Ar-H), 7.35 (s, 4H, Ar-H), 8.34 (s, 1H, NH); ^{13}C-NMR (DMSO-d_6): δ_{ppm}= 16.87 (CH_3), 17.25 (CH_3), 19.03 (CH_3), 46.78 (CH_2N), 116.06 (2CH_{Ar}), 116.44 (CH_2=), 119.30 (Thiazole-C_5), 123.35 (Thiazole-$C_{5'}$), 124.21 (CH_{Ar}), 125.81 (2CH_{Ar}), 126.51 (2CH_{Ar}), 129.51 (2CH_{Ar}), 133.31 (CH=), 134.86 (C_{Ar}), 139.81 (C_{Ar}), 143.15 (C_{Ar}), 154.21 (Thiazole-C_4), 161.47 (Thiazole-$C_{4'}$), 168.29 (Thiazole-C_2), 168.96 (Thiazole-$C_{2'}$), 172.75 (C=N); Anal. Calcd. for $C_{25}H_{24}BrN_7S_2$ (566.55): C,53.00; H, 4.27; N, 17.31%, Found: C, 53.01; H, 4.24; N, 17.29%.

2-Allylamino-4-methyl-5-(1-((4-methyl-3-phenyl-5-(4-ethoxyphenylazo)thiazol-2(3H)yildene) hydrazono)ethyl)thiazole (D). Orange powder, Yield (86%), mp 179-180ºC; IR (KBr) ν_{max}/cm^{-1}: 3198 (NH), 3068 (CH-sp^2), 2970 (CH-sp^3), 1622 (C=C), 1614 (C=N), 1567 (N=N); ^{1}H-NMR (DMSO-d_6): δ_{ppm} = 1.06 (t, *J* = 7.2 Hz, 3H, CH_3), 2.47 (s, 3H, CH_3), 2.52 (s, 3H, CH_3), 2.56 (s, 3H, CH_3), 3.92 (bs, 2H, NCH_2), 4.35 (q, J = 7.2 Hz, 2H, OCH_2), 5.15 (dd, J_{AB} = 1.5, J_{AC}= 10.2 Hz, 1H, =C-H_A), 5.26 (dd, J_{AB} = 1.5 Hz, J_{BC}=16.5Hz, 1H, =C-H_B), 5.87-5.96 (m, 1H, CH=), 6.91-7.20 (m, 5H, Ar-H), 7.44 (d, *J* = 7.8 Hz, 2H, Ar-$H_{3,5}$), 7.78 (d, *J* = 7.8 Hz, 2H, Ar-$H_{2,6}$), 8.35 (bs, 1H, NH); ^{13}C-NMR (DMSO-d_6): δ_{ppm}= 16.92 (CH_3), 17.36 (CH_3), 19.02 (CH_3), 19.70 (CH_3), 46.80 (CH_2N), 56.51 (OCH_2), 114.08 (Thiazole-C_5), 116.45 (CH_2=), 119.26 (Thiazole-$C_{5'}$), 123.51 (2CH_{Ar}), 126.35 (CH_{Ar}), 127.77 (2CH_{Ar}), 129.88 (2CH_{Ar}), 130.11 (2CH_{Ar}), 134.83 (CH=), 137.07 (C_{Ar}), 141.26 (C_{Ar}), 146.84 (C_{Ar}), 154.49 (Thiazole-C_4), 161.80 (Thiazole-$C_{4'}$), 168.10 (Thiazole-C_2), 169.06 (Thiazole-$C_{2'}$), 174.08 (C=N); Anal. Calcd. for $C_{27}H_{29}N_7OS_2$ (531.71): C,60.99; H, 5.50; N, 18.44%, Found: C, 60.96; H, 5.48; N, 18.41%.

2-Allylamino-4-methyl-5-(1-((4-methyl-3-phenyl-5-(4-sulfonamidophenylazo)thiazol-2(3H)yildene) hydrazono)ethyl)thiazole (E). Red crystals, Yield (87%), mp 177-178ºC; IR (KBr) ν_{max}/cm^{-1}: 3231, 3166 (NH_2), 3081 (NH), 3054 (CH-sp^2), 2981 (CH-sp^3), 1620 (C=C), 1596 (C=N), 1582 (N=N); ^{1}H-NMR (DMSO-d_6): δ_{ppm} = 2.47 (s, 3H, CH_3), 2.49 (s, 3H, CH_3), 2.57 (s, 3H, CH_3), 3.92 (bs, 2H, NCH_2), 5.16 (dd, J_{AB} = 1.5, J_{AC}= 10.2 Hz, 1H, =C-H_A), 5.26 (dd, J_{AB} = 1.5, J_{BC}=17.0 Hz, 1H, =C-H_B), 5.88-5.96 (m, 1H, CH=), 6.92-7.19 (m, 5H, Ar-H), 7.22 (s, 2H, NH_2), 7.44 (d, *J* = 8.5 Hz, 2H, Ar-$H_{3,5}$), 7.78 (d, *J* = 8.5 Hz, 2H, Ar-$H_{2,6}$), 8.35 (bs, 1H, NH); ^{13}C-NMR (DMSO-d_6): δ_{ppm}= 17.36 (CH_3), 19.02 (CH_3), 19.70 (CH_3), 46.81 (CH_2N), 114.08 (Thiazole-C_5), 116.45 (CH_2=), 119.26 (Thiazole-$C_{5'}$), 124.51 (2CH_{Ar}), 127.77 (2CH_{Ar}), 128.55 (2CH_{Ar}), 129.12 (CH_{Ar}), 129.98 (CH_{Ar}), 134.03 (CH=), 137.07 (C_{Ar}), 141.26 (C_{Ar}), 146.84 (C_{Ar}), 154.49 (Thiazole-C_4), 161.80 (Thiazole-$C_{4'}$), 168.10 (Thiazole-C_2), 169.06 (Thiazole-$C_{2'}$), 176.96 (C=N); Anal. Calcd. for $C_{25}H_{26}N_8O_2S_3$ (566.71): C,52.98; H, 4.62; N, 19.77%, Found: C, 52.95; H, 4.60; N, 19.75%.

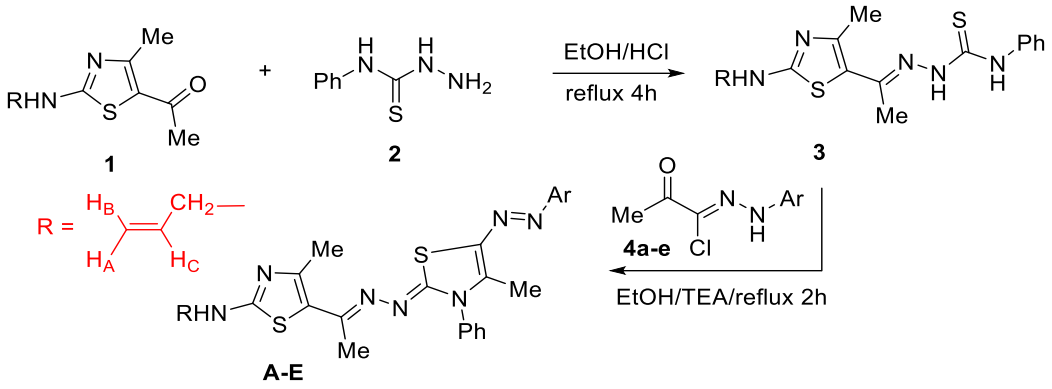

A, Ar = 4-F-C_6H_4-; B, Ar = 4-Cl-C_6H_4-; C, Ar = 4-Br-C_6H_4-; D, Ar = 4-EtO-C_6H_4-; E, Ar = 4-NH_2SO_2-C_6H_4-

Scheme 1. Synthesis of 2-allylamino-4-methyl-5-(1-((4-methyl--3-phenyl-5-(arylazo)thiazol-2(3H)ylidene)hydrazono)ethyl)thiazole derivatives ,**A-E**.

THEORETICAL IMPLEMENTATION

Kinetics

Significant thermodynamic parameters were computed over main decomposition stage in each compound under different heating rates beside the activation energy (E) and order (n). Many researches had established mathematical equations for this purpose and clarified their scientific meaning [30-38]. The rate of decomposition (equation 1) is the yield of two separated indices (k(T) and f(α)):

$$\frac{d\alpha}{dt} = k(T)\, f(\alpha) \qquad (1)$$

Therein, α is a fraction decomposed at time t, f(α) is a conversion function and k(T) is a temperature dependent function. The two functions are of Arrhenius type (equation 2):

$$K = A\, e^{-E^*/RT} \qquad (2)$$

Therein, R is the gas constant (J $mol^{-1}k^{-1}$). Using equation 2 as a function of equation 1, equation (3) was obtained:

$$\frac{d\alpha}{dT} = \left(\frac{A}{\varphi\, e^{-E^*/RT}}\right) f(\alpha) \qquad (3)$$

Therein, φ is the linear heating rate (dT/dt). Applying integration and approximation, equation (4) was obtained:

$$\ln g(\alpha) = \frac{-E^*}{RT} + \ln\left[\frac{AR}{\varphi E^*}\right] \qquad (4)$$

g(α) function depends on the mechanism of action in the decomposition process. Implementing Coat-Redfern [32] and Horowitz-Metzger methods [37], the temperature integral (right-hand side) and significant kinetics were evaluated.

Geometrical optimization

Applying DFT/B3LYP method using Gaussian 09 software [39], the optimized geometrical forms of arylazo-bithiazolylhydrazone derivatives were built (figure 1). 6-31G is a suitable base set for this purpose. Essential physical parameters which reflect significant features around the treated compounds were computed based on frontier energy gapes by known relations [40, 41] as follows:

1- $\chi = -0.5\,(E_{LUMO} + E_{HOMO})$
2- $\mu = -\chi = 0.5\,(E_{LUMO} + E_{HOMO})$
3- $\eta = 0.5\,(E_{LUMO} - E_{HOMO})$
4- $S = -0.5\,\eta$
5- $\omega = \mu^2/2\,\eta$
6- $\sigma = 1/\eta$

Two considerable files (log and chk) were excreted. The files were visualized over Gauss program screen [42] to obtain essential physical data.

QSAR parameters computation

Surface area, volume, hydration energy, log P, reactivity and polarizability were the calculated QSAR parameters over optimized structures (A-E). The optimization process was executed by HyperChem (8.1) program. Semi-empirical AM1 followed by molecular mechanics (MM^+) were the suitable setup methods before the geometrical optimization process. The optimization process was accomplished without restriction for any parameters, after which the parameters were computed separately [43].

Molecular docking process

This is a recent computational method in drug designing industry as a preliminary test of the inhibition efficiency of organic compounds towards pathogen protein. Auto Dock tool 4.2 was implemented for docking process between arylazo-bithiazolylhydrazone derivatives and calf thymus DNA (2hio). Non-polar hydrogen atoms were added and the rotatable bonds were excluded before. Fundamental hydrogen atoms, charges (Kollman united) and solubility parameters were then added [44]. The affinity (grid) maps of ×× Å grid points and 0.375 Å spacing were obtained through Autogrid program [45].

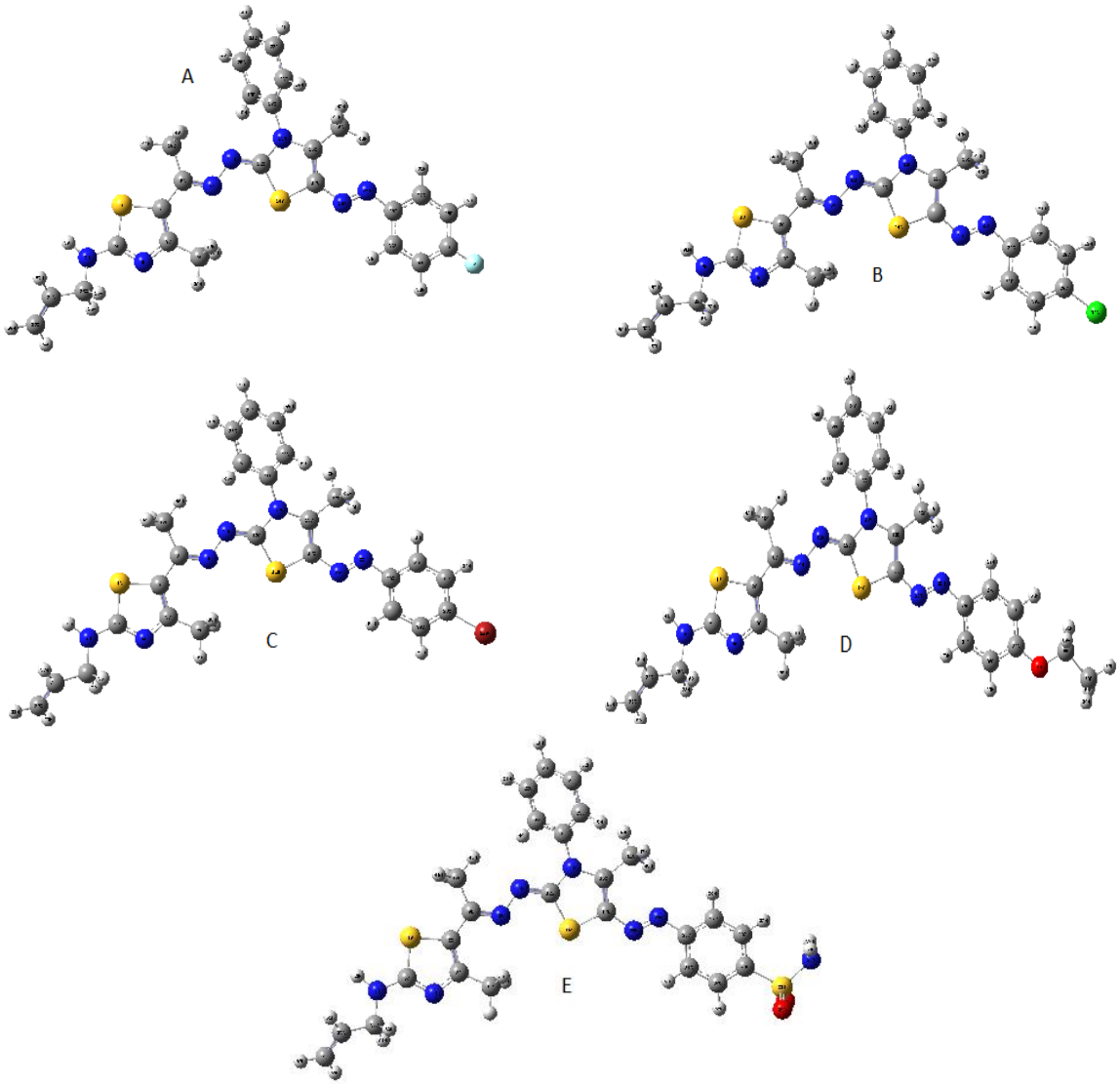

Fig. 1. The optimized structures of arylazobithiazolylhydrazone derivatives (A-E).

Electrostatic terms and van der Waals forces were estimated through dielectric function (distance-dependant) and auto dock parameter set, respectively. Docking process was executed by Solis & Wets local search method and Lamarckian genetic algorithm (LGA) [46]. The orientation, initial position and torsions of tested molecules were set incidentally. All rotatable torsions were decomposed during the docking process. Each experiment was the average value of 10 different runs which set to close after maximum of 250000 energy assessments. The used population size was 150. During the process, in the translational step (0.2 Å) quaternion and torsion steps were applied.

RESULTS AND DISCUSSION

Mechanism of action

As outlined in scheme 1, 1-(2-allylamino-4-methylthiazol-5-yl) ethanone (**1**) was condensed with 4-phenylthiosemicarbazide (**2**) in ethanol (boiling) containing HCl as a catalyst to afford thiazolylthiosemicarbazone **3** in good yield. The

chemical structure of compound **3** was built based on elemental analysis, spectral data, and chemical transformations. The IR spectrum of compound **3** exhibited absorption bands at 3310, 3187, 3036, 1622, 1598, and 1261 cm^{-1} characteristic to three NH, C=C, C=N, and C=S groups, respectively. Its ^{1}H-NMR spectrum revealed, besides the expected signals of phenyl and allyl protons, two singlets at δ 2.38 and 2.52 ppm assignable to two methyl protons, and three broad singlet signals, exchangeable with D_2O, at δ 9.81, 10.43, 11.08 ppm owing to three NH protons. The ^{13}C-NMR spectrum of compound **3** revealed the presence of fourteen carbon signals compatible with its molecular formula ($C_{16}H_{19}N_5S_2$). The most characteristic carbon signals resonate at δ 14.78, 16.66, 47.93, 177.03 ppm owing to two methyl carbons, methylene, and thiocarbonyl group, respectively.

Next, we investigated the reactivity of the thiourea moiety in compound **3** towards hydrazonoyl chlorides with the aim to attain arylazobithiazolylhydrazones for thermal analysis investigation. Thus, reaction of compound **3** with a series of *N*-aryl hydrazonoyl chlorides **4a-e** [29] in boiling ethanol containing triethylamine as a basic catalyst gave one isolable product in each case (as evidenced by TLC analysis of the crude product), which were recognized to be products **5a-e** (Scheme 1). The structure of products **5a-e** was confirmed by elemental analyses and spectral data. The IR spectra of products **5a-e** showed in each case the disappearance of C=S absorption band and the presence of new absorption bands in the ranges 1592-1598 and 1567-1582 cm^{-1} assigned to conjugated C=N and N=N groups, respectively. The ^{1}H-NMR spectrum of compound **5d**, as an example, revealed in addition to the expected signals of the allyl amino protons, aromatic protons, and protons of three methyl groups, a triplet signal at δ 1.06 ppm and a quartet signal at 4.35 ppm assigned to ethoxy group. There is also a pair of doublet signals resonating around 7.44, 7.78 ppm with the same coupling constant value (*J* = 7.8 Hz) assigned to the four protons of p-substituted benzene ring residue. The ^{13}C-NMR spectrum of compound **5d** revealed the presence of 23 carbon signals. The sp^3 hybridized carbon atoms resonate at δ 16.92, 17.36, 19.02, 19.70, 46.80 and 56.51 ppm characteristic to four methyl carbons, CH_2N, and OCH_2, respectively. The more downfield three carbons resonate at δ 168.10, 169.06, 174.08 ppm assigned to the carbons of thiazole-C_2, thiazole-$C_{2'}$, and C=N, respectively (see supplementary data). The mass spectra of all products **5a-e** exhibited in each case a molecular ion peak at the correct molecular weight for the respective compound (see Experimental). To account for the formation of products **5a-e**, it was suggested that the reaction starts *via* nucleophilic attack of the thiol group in compound **3** to the electron-deficient carbon of the hydrazone group in compounds **4a-e** and subsequent *in situ* dehydrative cyclization to give the target products **5a-e**.

TGA homolysis of arylazobithiazolylhydrazone derivatives

Although an observable shortage in researches concerning the relation between p-substituents and the thermal behavior of compounds, some articles exhibited essential knowledge about their pyrolysis [47-49]. All derivatives were subjected to thermal analysis (TGA and DTG) up to 800°C (figure 2). The data (Tables 1&S1-S4) show discriminate findings in mass loss for all compounds (A-E) which were recorded with heating rate variations (5-25 K. min^{-1}) although the high similarity in homolysis pathway in various derivatives observable distinct features toward thermal stability which clearly appeared in the first stage of pyrolysis. These observations clarify the high impact of heating rate changes, as well as p-substituents. The substituents with high inductive effect led to difficult degradation over the whole molecule. This reflected on incomplete pyrolysis of the organic compounds. Derivative A displayed high rigidity in the pyrolysis process in agreement with the high inductive effect of the small-sized substituent (F) followed by derivative D for OC_2H_5 substituent.

Kinetic studies

This part in our research is considered the most significant, in which the study is being processed to estimate the kinetic parameters. The kinetic parameters (ΔH, ΔG and ΔS) and energy of activation were estimated by using two comparative reference equations [32, 37]. These calculated parameters serve for discrimination of the influence of changeable substituents on the degree of thermal rigidity. Moreover, the parameters were calculated under variable heating rates (5-25 K.min^{-1}) to investigate the degree of shifts in their values in coinciding. Figure 3 displays relations for Coat-Redfern and Horowitz-Metzger methods under various conditions (heating rate and *p*-substituents). The data were computed by applying two methods (Tables 2&S5-S8) over most suitable degradation stage (second and sometimes the first). This stage accidently the main degradation stage represents expel of a great mass.

The first view of the relations (figure 3) showed the mismatch of the resulting lines, which confirms the effect of the substituents on the behavior of thermal decomposition for compounds and also on the effect of changes in the heating rate. The data demonstrated that there are many reactions; number of reactions is increasing at low heating rates (5 and 10 K. min^{-1}) compared to high rates (15-25 K. min^{-1}). Although, only one effective reaction was taken in consideration for simplicity and the parameters are displayed in the tables reported. It is noted that all pyrolysis models are based on a single effective reaction. Moreover, there is an observable increase of kinetic parameters values with increasing heating rate. Also, the high inductive effect of the substituents leads to high values of the kinetic parameters as appeared in A, B and D compounds for F, Cl and OC_2H_5 p-substituents.

Structural optimization process. DFT/B3LYP method

The best atomic distribution inside the five derivatives (figure 1) was obtained in gas phase by DFT/B3LYP method with 6-31G base set. The frontier energy gaps (E_{HOMO} - E_{LUMO}) were calculated and used for computing other significant parameters (Table 3) using reference relations [50, 51]. Electronegativity index (χ), chemical potential index (μ), global hardness index (η), global softness index (S), global electrophilicity index (ω) and absolute softness (σ) were the parameters computed. Electrophilicity parameter is indicator for the degree of reactivity and toxicity for the tested compound. Electronic chemical potential (μ) and electronegativity (χ) are two opposite faces pointing at the degree electron affinity gained from universe. Global hardness (η), global softness (S) indices are also two opposite faces pointing to the degree of flexibility of the compound which serve to distinguish the biological behavior of the compound inside the cell. All indices introduce distinguished reactivity and toxicity of compound E, which includes substituent SO_2NH_2.

Table 1. Plausible degradation process for arylazobithiazolylhydrazones (at 5 K. min^{-1} heating rate)

Compound	Steps	Temp. range (°C)	Decomposed	Weight loss: Calcd (Found) (%)
A	1st	50.2-81.4	CH_4	3.17(3.17)
	2nd	200.1-308.4	$C_7H_8N_4S$	35.64(35.67)
	3rd	362.4-515.1	$C_5H_{12}N_3SF$	32.68(32.71)
	Residue		12C	28.50(28.45)
B	1st	51.2-91.1	$C_7H_9N_2S$	29.35(30.00)
	2nd	122.6-301.2	$C_9H_8N_3$	30.30(30.41)
	3rd	305.6-400.1	$C_6H_7N_2ClS$	33.45(33.61)
	Residue		3C	6.90(5.98)
C	1st	55.1-170.2	$C_9H_{11}N_2S$	31.64(31.65)
	2nd	221.5-452.1	$C_{16}H_{11}N_5Br$	62.34(62.33)
	3rd	535.2-581.3	H_2S	6.02(6.02)
	Residue		nil	
D	1st	122.3-305.4	$C_{25}H_{25}N_7OS_2$	94.72(94.75)
	2nd	350.2-403.3	C_2H_4	5.28 (5.25)
	Residue		nil	
E	1st	61.2-122.1	C_3H_6N	9.80(9.81)
	2nd	210.1-341.2	$C_{13}H_{11}N_4S$	45.05(45.04)
	3rd	420.3-583.2	$C_3H_2N_2S$	17.31(17.33)
	Residue		$C_6H_7SO_2N$	27.74(27.82)

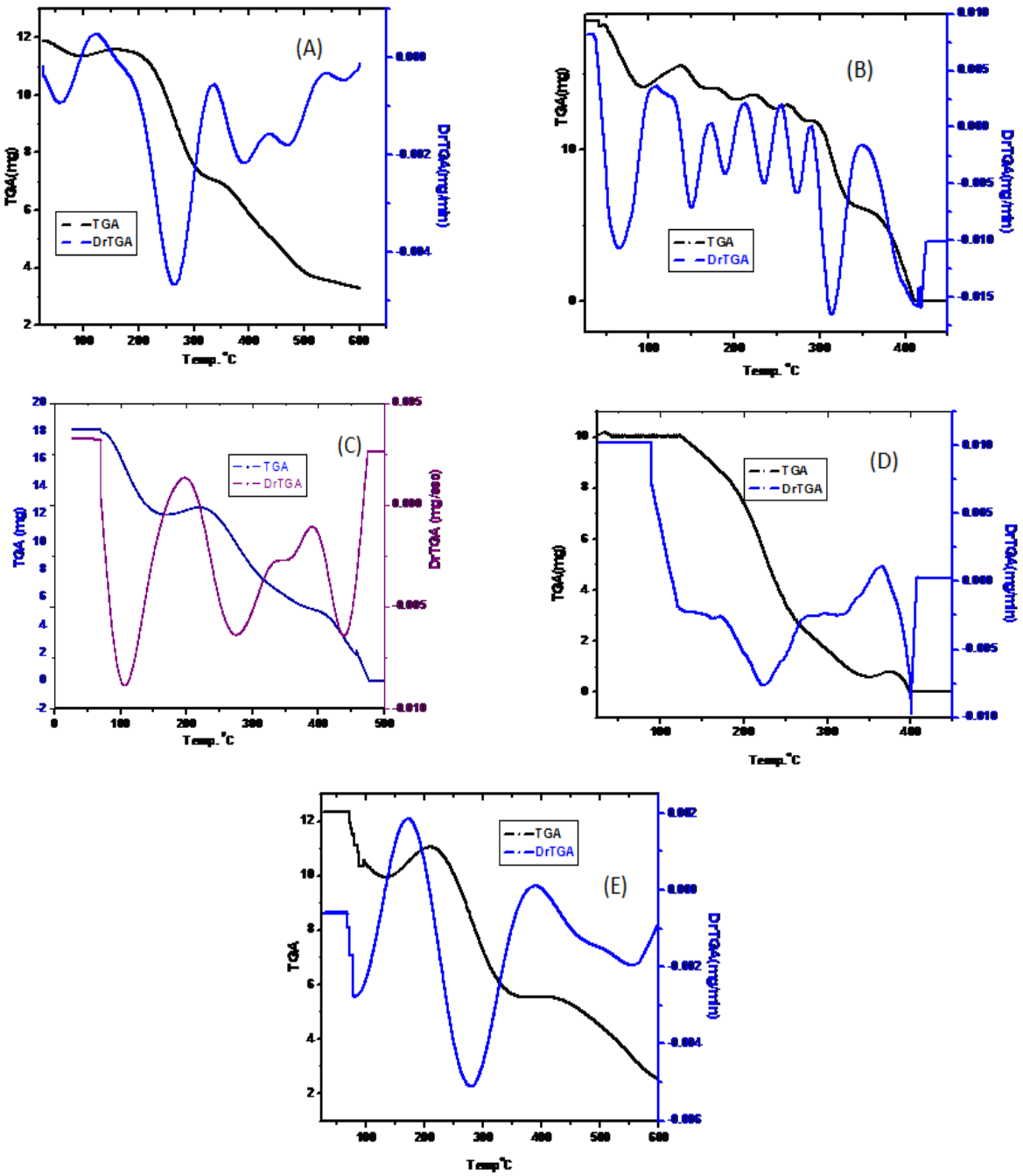

Fig. 2. TGA and DTG of compounds A-E at 5 K. min $^{-1}$ heating rate

Table 2. Computed kinetic parameters by Coats–Redfern (CR) and Horowitz–Metzger (HM) (for main step at 5 K min $^{-1}$ heating rate)

Comp.	Step	Method	Kinetic Parameters					
			E (Jmol^{-1})	A (S^{-1})	ΔS(Jmol^{-1}K^{-1})	Δ H (Jmol^{-1})	Δ G (Jmol^{-1})	r
A	2nd	CR	4.25E+04	7.05E+03	-1.76E+02	5.82E+04	1.51E+05	0.9993
		HM	5.96E+04	5.90E+04	-1.58E+02	6.52E+04	1.49E+05	0.9991
B	2nd	CR	2.69E+04	2.06E+01	-2.24E+02	3.29E+04	1.41E+05	0.9993
		HM	4.37E+04	2.80E+02	-2.02E+02	3.96E+04	1.38E+05	0.9991
C	2nd	CR	3.73E+04	3.77E+00	-2.40E+02	3.22E+04	1.78E+05	0.9993
		HM	4.87E+04	5.86E+01	-2.17E+02	4.37E+04	1.76E+05	0.9991
D	2nd	CR	4.01E+04	1.40E+04	1.94E+01	1.96E+04	1.83E+05	0.9993
		HM	4.11E+04	1.48E+4	3.90E+01	2.06E+04	1.81E+05	0.9991
E	2nd	CR	3.51E+04	8.54E+03	-1.75E+02	6.05E+04	1.56E+05	0.9993
		HM	4.27E+04	6.06E+04	-1.58E+02	6.82E+04	1.55E+05	0.9991

Table 3. Computational parameters of arylazobithiazolylhydrazones through DFT/B3LYP method

Comp.	E_H (eV)	EL (eV)	EH - EL) (eV)	El-Eh	*x*(eV)	μ(eV)	η(eV)	S(eV-1)	ω(eV)	σ(eV)
A	-0.17306	-0.08827	-0.0848	0.08479	0.130665	-0.13067	0.042395	0.021198	0.20136	23.58768723
B	-0.17606	-0.08905	-0.087	0.08701	0.132555	-0.13256	0.043505	0.021753	0.20194	22.98586369
C	-0.17539	-0.08876	-0.0866	0.08663	0.132075	-0.13208	0.043315	0.021658	0.20136	23.08669052
D	-0.16986	-0.07713	-0.0927	0.09273	0.123495	-0.1235	0.046365	0.023183	0.164467	21.5679931
E	-0.18289	-0.10579	-0.0771	0.0771	0.14434	-0.14434	0.03855	0.019275	0.270221	25.94033722

Table 4. Estimated physical parameters extracted from log files

Comp.	Dipole moment, D (Debye)	Oscillator strength, ∫	Excitation energy, E (nm)	Heat of formation, E (A.U.)	Charge of p-substituent C^{29}
A	3.6863	0.2439	633.03	-2245.95315356	0.315047
B	4.6705	0.3433	599.73	-2606.32416645	-0.280876
C	4.3800	0.3488	603.2	-4717.72566804	-0.316959
D	3.9918	0.3666	565.56	-2300.54347509	0.318885
E	12.1981	0.3596	673.91	-2750.36357247	-0.238973

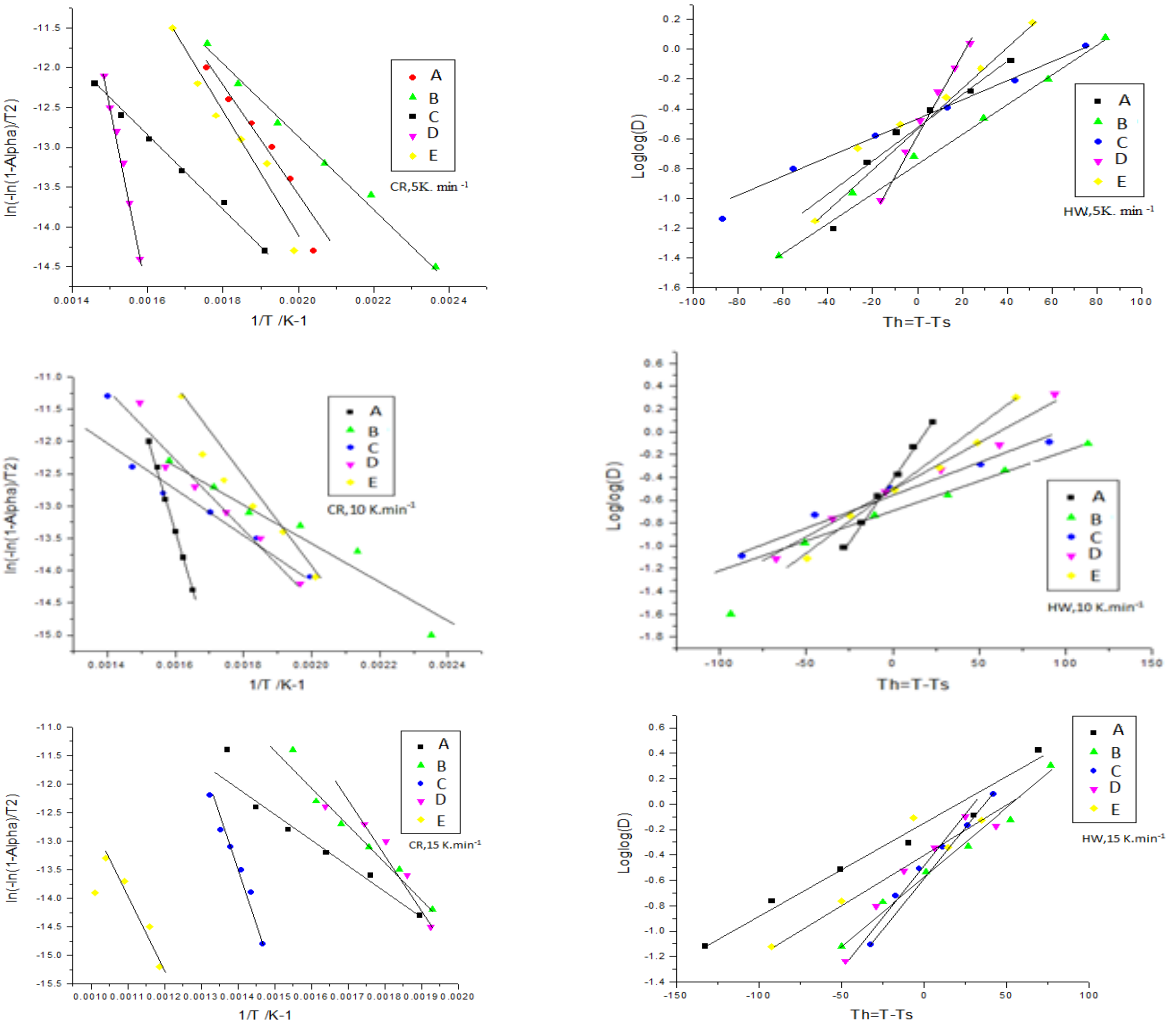

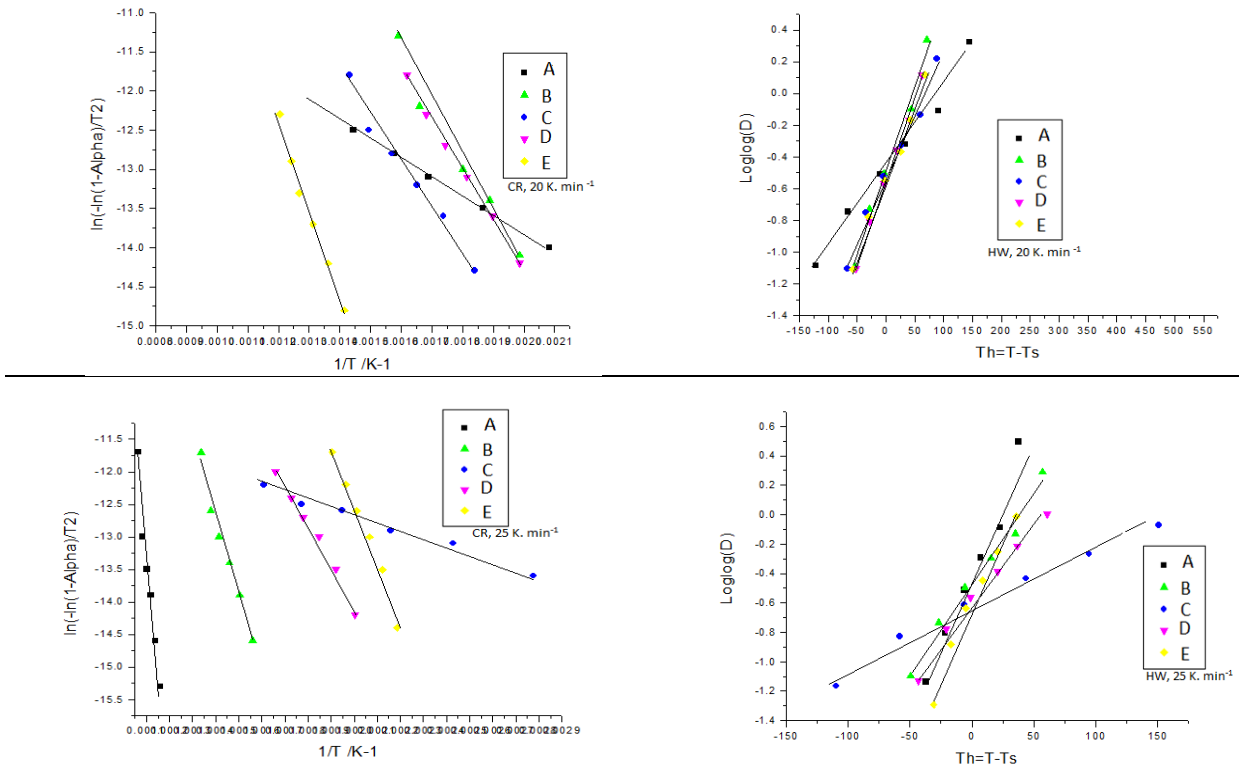

Fig. 3. The kinetic plots for Coats–Redfern (CR) and Horowitz–Metzger (HM) methods for main step in compounds (A-E) at various heating rates

Table 5. QSAR computational parameters for optimized new arylazobithiazolylhydrazone compounds

Function	**A**	**B**	**C**	**D**	**E**
Surface area (Approx) (Å^2)	691.61	716.75	725.66	774.24	749.95
Surface area (Grid) (Å^2)	793.77	823.25	835.76	882.42	871.61
Volume (Å^3)	1384.42	1418.55	1437.20	1512.01	1499.67
Hydration energy (Kcal/mol)	-14.26	-14.21	-14.18	-15.23	-20.47
Log P	3.84	4.21	4.49	3.79	2.58
Reactivity (Å^3)	159.32	163.91	166.73	170.32	172.45
Polarizability (Å^3)	55.30	57.32	58.02	59.70	57.88
Mass(amu)	505.63	522.09	566.54	531.69	566.71

Oscillator strength values fall in the known range (0-1) [52], which reflects the high probability for the absorption or emission of radiations during the transition between levels. The computed values fall near to each other's and show the flexibility in absorption and emission character for all molecules. Excitation energy values coincide with heat of formation which appeared high with compound E. The computed charges over the carbon atom, which bonds to substituents, point to variable attachments from ionic to covalent.

This is another type of parameters estimated upon optimized structures applying molecular mechanics (Table 5) of Hyper Chem (8.1) program. These parameters assert on the discrimination between derivatives under the effect of substituents. Surface area, volume, hydration energy, partition coefficient (log P has a reverse relation with biological susceptibility), reactivity and polarizability are essential parameters which give a clear insight about such influence. A marked difference between estimated values coincides with the effect of substituents. Estimated values of compound **E** showed its best qualities as regards reactivity and biological susceptibility [53].

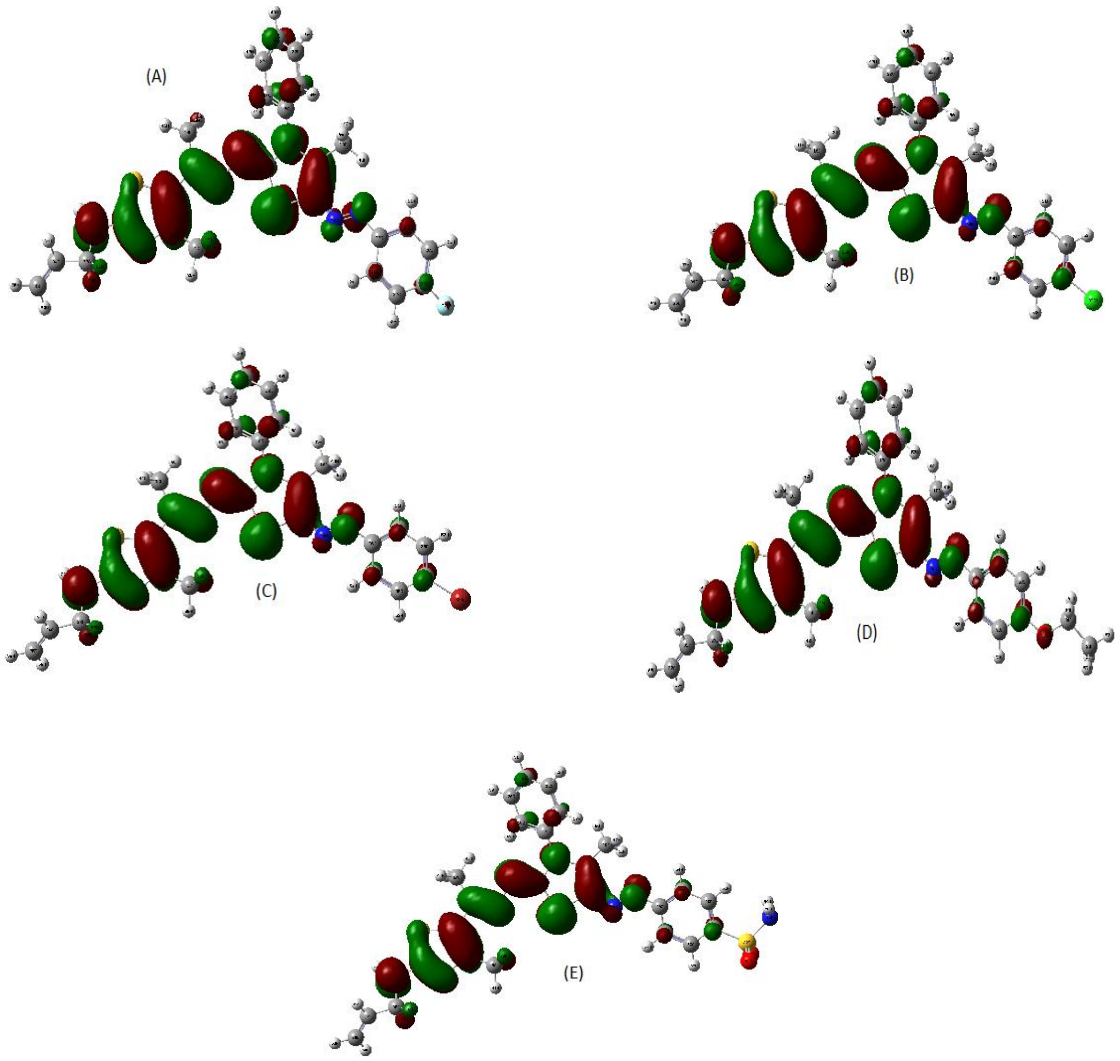

Fig. 4. Frontier HOMO level of arylazobithiazolylhydrazone derivatives (A-E)

QSAR calculations. Docking study

This study is considered the biggest revolution in computational study dealing with drug designing through simulation process. The docking process was executed for each derivative (A-E; as PDB file) against the calf thymus DNA protein (2hio) to give an insight about the degree of interaction in between. The DNA protein used was selected to simulate what may happen inside any infected cell. As we know that, the first target for any treatment drug, is the cell-DNA, so the interaction with DNA, may give the best view about treatment for many microbial diseases. The extracted parameters (Table 6) led to a clear view about the inhibition efficiency of tested compounds. The comparative vision for the data calculated displays a great differentiation between compounds (A-E) especially for values of inhibition constant calculated. Also, the data point to the priority of compound E among the others in agreement with previous computational studies. Such priority of the compound asserts on highly expected inhibition behavior towards pathogen and its success in the medical field. Figure 6 illustrates the complexes between proposed inhibitors and DNA protein receptor. The Hp and 2D plots introducing the same number of H-bonding were obtained with all complexes. Moreover, nitrogen no. 25 is the sponsor of intra-hydrogen bonding with the protein except for compound B. This compound represents a chloro-substituent, which has a negative effect on the donation feature of the atom (N^{25}) towards the H-bonding. Also, the best prolongation for the DNA helixes was observed with compound E, in agreement with previously reported data in this study.

CONCLUSION

This study is focusing on the effect of substituents on the features of organic compounds as: thermal, kinetic; stability, reactivity and biological suitability. The influence of *p*-substituents (F, Cl, Br, OC_2H_5 and SO_2NH_2) was stated from the thermal and kinetic study. The substituents which have a high inductive effect, led

to difficult degradation over the whole molecule. The type of reactions in degradation process was reduced by increasing heating rate. Also, the kinetic parameter values are directly attached with heating rates. The computational studies also assert on the great influence for the substituents on many significant features of the compound. The physical parameters calculated over optimized structures showed a great difference in between derivatives in coinciding with various substituents. The best features were obtained for derivative E which includes a highly inductive substituent (SO_2NH_2). Molecular docking against DNA was also tested and the inhibition energy parameters were estimated over docked complexes. Also, the inhibition activity was recorded with derivative E. So promising biological activity can be predicted with one derivative among all. This result asserted on the significant influence of substituents although the moiety of compounds used is fixed.

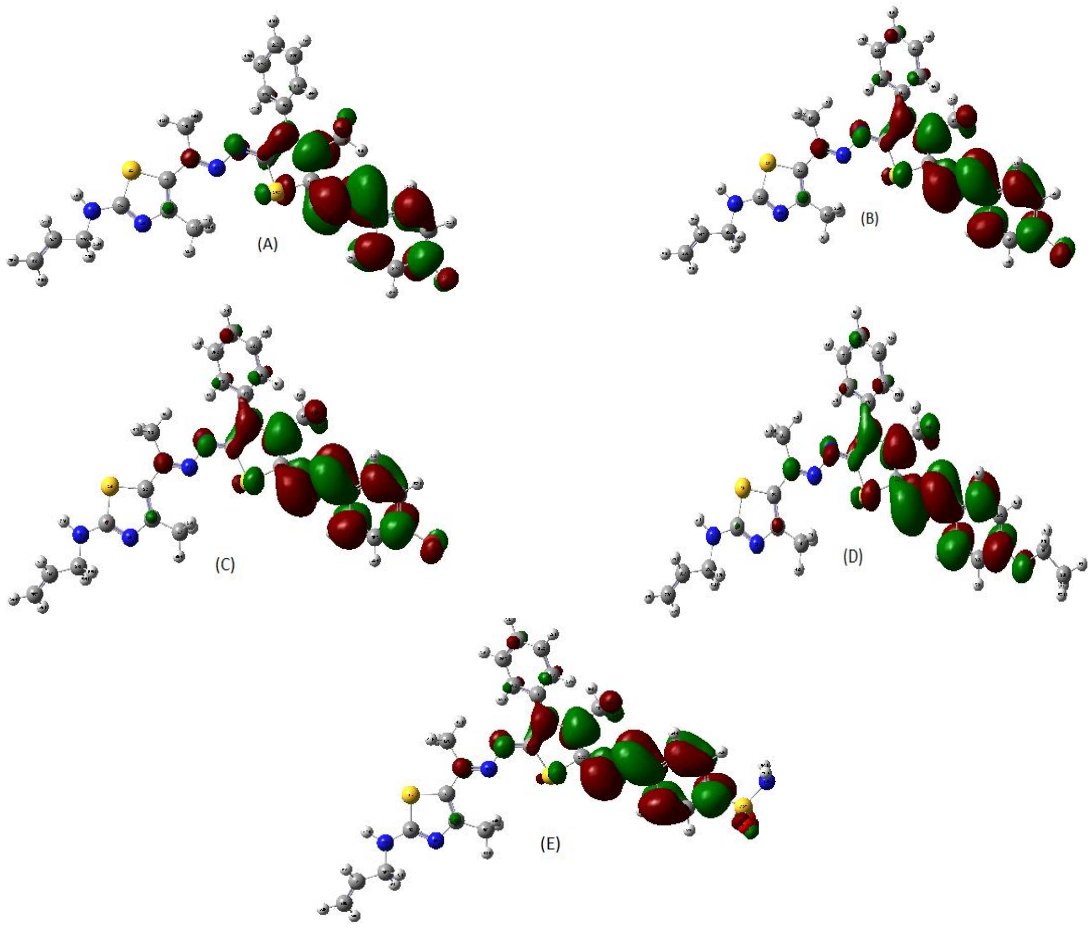

Fig. 5. Frontier LUMO level of arylazobithiazolylhydrazone derivatives (A-E).

Table 6. Docking energy values (k cal/mol) for new arylazobithiazolylhydrazones- DNA receptor (2hio) complexes

Comp.	Est. free energy of binding	Est. inhibition constant (K_i) (μM)	vdW+ bond+ desolve energy	Electrostatic energy	Total intercooled energy	Frequency	Interact surface
A	-6.28	24.72	-8.53	+0.03	-8.50	10%	1128.309
B	-6.82	10.10	-8.98	-0.12	-9.10	10%	1131.124
C	-6.07	35.31	-8.52	+0.06	-8.46	10%	1126.701
D	-6.13	32.17	-8.72	-0.10	-8.82	10%	1147.885
E	-5.86	50.34	-8.50	-0.04	-8.54	20%	1190.344

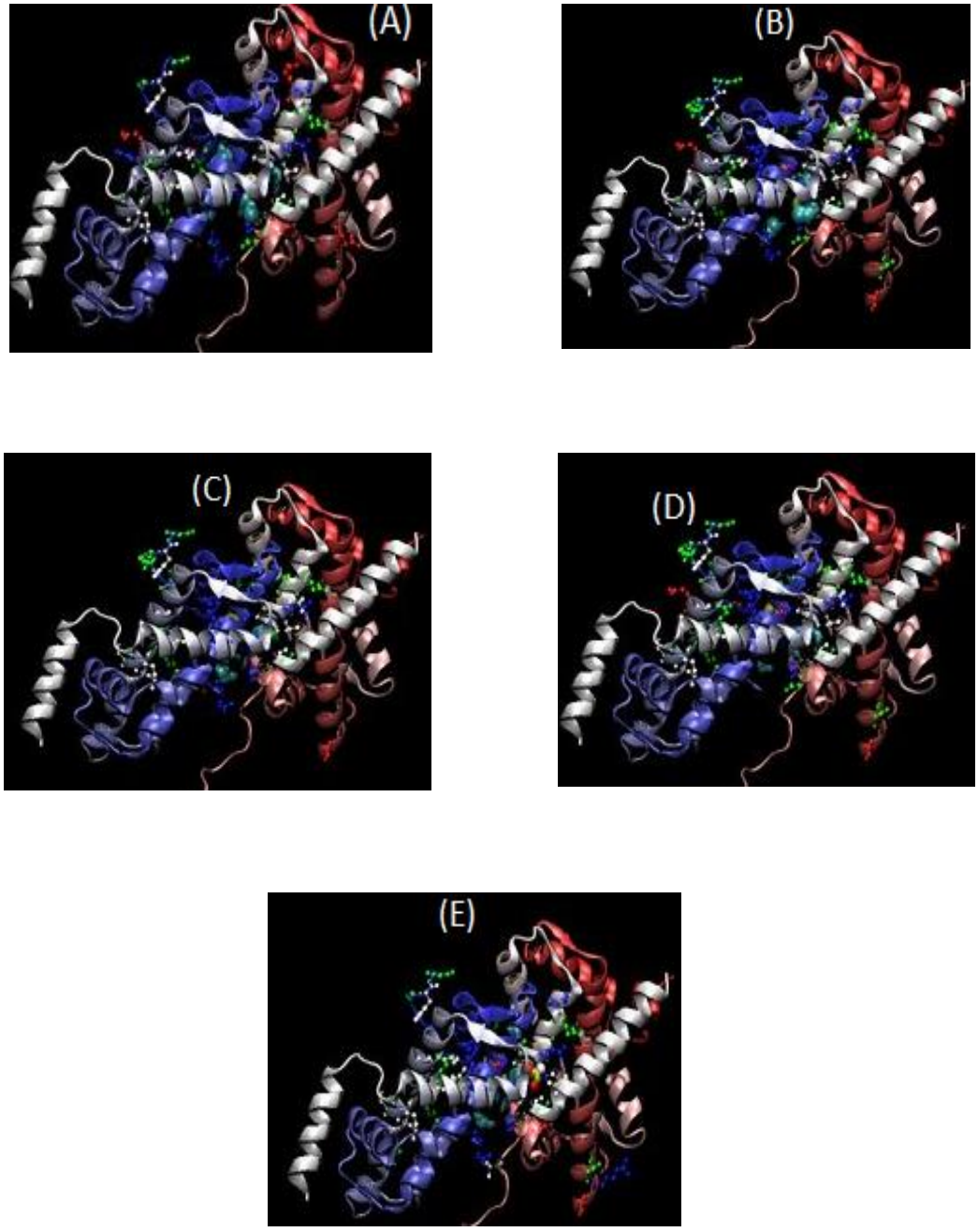

Fig. 6. The docking complexes of arylazobithiazolylhydrazone derivatives (A-E) with DNA protein receptor (2hio)

REFERENCES

1. W. Hussein, G.T. Zitouni, *MOJ Bioorg. Org. Chem*., **2**, 52 (2018).
2. N. Siddiqui, M.F. Arshad, W. Ahsan, M.S. Alam, *Int. J. Pharm. Sci. Drug. Res*., **1**, 136 (2009).
3. N. Singh, S.K. Bhati, A. Kumar, *Eur. J. Med. Chem.*, **43**, 2597 (2008).
4. N. Vasu, B.B.K. Goud, Y.B. Kumari, B. Rajitha, *Rasayan J. Chem*., **6**, 201 (2013).
5. G. Turan-Zitouni, P. Chevallet, F.S. Kilic, K. Erol, *Eur. J. Med. Chem*., **35**, 635 (2000).
6. E.L. Luzina, A.V. Popov, *Eur. J. Med. Chem.*, **44**, 4944 (2009).
7. R.K. Rawal, R. Tripathi, S.B. Katti, C. Pannecouque, E. De-Clercq, *Eur. J. Med. Chem*.,**43**, 2800 (2008).
8. T. Iino, D. Tsukahara, K. Kamata, K. Sasaki, S. Ohyama, H. Hosaka, T. Hasegawa, M. Chiba, Y. Nagata, J.Eiki, T. Nishimura, *Bioorg. Med. Chem*., **17**, 2733 (2009).
9. A. Satoh, Y. Nagatomi, Y. Hirata, S. Ito, G. Suzuki, T. Kimura, S. Maehara, H. Hikichi, A. Satow, M. Hata, H. Ohta, H. Kawamoto, *Bioorg. Med. Chem. Lett*., **19**, 5464 (2009).
10. G. Verma, A. Marella, M. Shaquiquzzaman, M. Akhtar, M.R. Ali, M.M. Alam, *J. Pharm. Bioallied Sci*., **6**, 69 (2014).

11. S. Rollas, S.G. Kucukguzel, *Molecules*, **12**, 1910 (2007).
12. I. Hussain, A. Ali, *J. Phytochemistry Biochem*., **1**, 1 (2017).
13. M. Abdelmotaal, A. Nabil, *European Chemical Bulletin*, **7**, 280 (2019).
14. G. Graser-Loescher, A. Schoenhuber, C. Ciglenec, S. Eberl, G. Krupitza, R.M. Mader, S.S. Jadav, V. Jayaprakash, M. Fritzer-Szekeres, T. Szekeres, P. Saiko, *Food Chem. Toxicol*., **108**, 53(2017).
15. C. Boldron, I. Van der Auwera, C. Deraeve, H. Gornitzka, S. Wera, M. Pitié, F. Van Leuven, B. Meunier, *ChemBioChem*., **6**, 1976 (2005).
16. S. Ayton, P. Lei, A.I. Bush, *Free Radic. Biol. Med*., **62**, 76 (2013).
17. L.N. Suvarapu, A.R. Somala, J.R. Koduru, S.O. Baek, V.R. Ammireddy, *Asian J. Chem*., **24**, 1889 (2012).
18. B.B. Holló, J. Magyari, S. Armaković, G.A. Bogdanović, M.V. Rodić, S. J. Armaković, J. Molnár, G. Spengler, V. M. Leovac, K.M. Szécsényi, *New J. Chem.*, **40**, 5885 (2016).
19. S.S. Kumar, S.Biju, V. Sadasivan, *J. Mol. Struc*., **1156**, 201 (2018).
20. A.B. Thomas, R.K. Nanda, L.P. Kothapalli, S.C. Hamane, *Arab. J. Chem*., **9**, 79 (2016).
21. I.H. Hall, S.Y. Chen, K.G. Rajendran, D.X. West, *Appl. Organomet. Chem.*, **10**, 485 (1996).
22. U. Kulandaivelu, V.G. Padmini, K. Suneetha, J.V. Vidyasagar, T.R. Rao, K.N. Jayaveera, A.Basu, V. Jayaprakash, *Arch. Pharm*., **344**, 84 (2011).
23. N.A. Mohamed, R.R. Mohamed, R.S., Seoudi, *Int. J. Biol. Macromol*., **63**, 163 (2014).
24. A. Bartyzel, *J. Therm. Anal. Calorim*., **131**, 1221 (2018).
25. M.N. Patel, N. H. Patel, P.K. Panchal, D.H. Patel, *Synth. React. Inorg. Met. Org. Nano Met. Chem*., **34**, 873 (2004).
26. V. K. Aghera, P.H. Parsania, *J. Sci. Ind. Res*. **67**, 1083 (2008).
27. B.J. Gangani, J.P. Patel, P.H. Parsania, *Russian J. Phys. Chem*. A, **89**, 2367 (2015).
28. S. Bondock, A.M. Fouda, *Synth. Commun*., **48**, 561 (2018).
29. I. Althagafi, M.G.Elghalban, F.A.Saad, J.H. Al-Fahemi, N.M. El-Metwally, S. Bondock, L. Almazroai, K.A. Saleh, G.A. Al-Hazmi, *J. Mol. Liq*., **242**, 662 (2017).
30. G.A. Bain, J.F. Berry, Diamagnetic Corrections and Pascal's Constants, *J. Chem. Educ*., **85,** 532 (2008).
31. E.S. Freeman, B. Carroll, *J. Phys. Chem*., **62**, 394 (1958).
32. A.W. Coats, J.P. Redfern, *Nature*, **201**, 68(1964).
33. T. Ozawa, *Bull. Chem. Soc. Japan*, **38**, 1881 (1965).
34. W.W.Wendlandt, Thermal Methods of Analysis, New York, Wiley, 1974.
35. J.H. Flynn, *J. Therm. Anal. Calorim*., **27**, 95 (1983).
36. P. Kofstad, *Nature*, **179**, 1362 (1957).
37. H.W. Horowitz, G.A. Metzger, *Anal. Chem*., **35**, 1464 (1963).
38. X. Wu., A.K. Ray, *Phys. Rev. B*., **65**, 85403(2002).
39. M. J. Frisch et al., Gaussian 09, Revision D, Gaussian Inc., Wallingford, CT (2010).
40. R.K. Ray, G.R. Kauffman, *Inorg. Chem. Acta*, **173**, 207 (1990).
41. R.C. Chikate, S.B. Padhye, *Polyhedron*, **24**, 1689 (2005).
42. R. Dennington, T. Keith, J. Millam .Gauss View, Version 4.1.2, SemichemInc, Shawnee Mission, KS, 2007.
43. M.M. Al-Iede, J. Karpelowsky, D.A. Fitzgerald, *Pediatr. Pulmonol*., **51**, 394 (2016).
44. T.A. Halgren, *J. Comput. Chem*., **17**, 490 (1998).
45. G.M. Morris, D.S. Goodsell, R.S. Halliday, R. Huey, W.E. Hart, R.K. Belew, A.J. Olson, *J. Comput. Chem.*, **19**, 1639 (1998).
46. D.S. Solis, R.J.B. Wets, *Math. Oper. Res*., **6**, 19 (1981).
47. M.A. Sheraz, S.H. Kazi, S. Ahmed, Z. Anwar, I. Ahmad, *Beilstein J. Org. Chem*., **10**, 1999 (2014).
48. Z. Razaczynska, A. Danczowska-Burdon, J. Sienkiewicz-Gromiuk, *J. Therm. Anal. Calorim*., **101**, 671 (2010).
49. M. Juha´sz, Y. Kitahara, S. Takahashi, T. Fujii, *Anal. Lett*., **45**, 1519 (2012).
50. U. El-Ayaan, N.M. El-Metwally, M.M. Youssef, S. A.A. El Bialy, *Spectrochim. Acta A*, **68**, 1278 (2007).
51. S.K. Tripathi, R. Muttineni, S.K. Singh, *J. Theor. Biol*., **334**, 87 (2013).
52. C. Fosset, B.A. McGaw, M.D. Reid, *J. Inorg. Biochem*., **99**, 1018 (2005).
53. N. Terakado, S. Shintani, Y. Nakahara, *Oncol. Rep*., 7, 1113 (2000).